In situ AFM study of pitting corrosion and corrosion under strain on a 304L stainless steel

F.A. Martin[a], J. Cousty[b,*], J-L. Masson[b], C. Bataillon[c]

[a]*CEA de Saclay DRECAM/SPCSI, 91191 Gif-sur-Yvette cedex, frantz.martin@cea.fr*
[b] *CEA de Saclay DRECAM/SPCSI, 91191 Gif-sur-Yvette cedex, cousty@cea.fr*
[c]*CEA de Saclay DEN/DPC/LECA, 91191 Gif-sur-Yvette cedex, christian.bataillon@cea.fr*

ABSTRACT

Our study is centred on surface localised corrosion under strain of a standard stainless steel (304L). The interest we take in these corrosion phenomena is led by the general misunderstanding of its primary initiation steps. The goal of this study is to determine precisely the relationships between local geometrical defects (grain boundaries, dislocation lines…) or chemical defects (inclusions) with the preferential sites of corrosion on the strained material.

By combining three techniques at the same time: Atomic Force Microscopy, an electrochemical cell and a traction plate, we can observe in situ the effect of localised stress and deformation on the sample surface exposed to a corrosive solution.

We managed to build an original set-up compatible with all the requirements of these three different techniques.

Furthermore, we prepared the surface of our sample as flat as possible to decrease at maximum the topographical noise in order to observe the smallest defect on the surface. By using a colloidal suspension of SiO_2, we obtained surfaces with a typical corrugation (RMS) of about 1 Å for areas of at least 1 µm².

Our experimental study has been organised in two primary investigations:

- ✓ In situ study of the morphology evolution of the surface under a corrosive chloride solution (borate buffer with NaCl salt). The influence of time, NaCl concentration, and potential was investigated.

- ✓ In situ exploration of a 304L strained surface. It revealed the first stages of the surface plastic evolutions like activation of sliding dislocations, materialised by parallel steps of about 2 nm high in the same grain. The secondary sliding plane systems were also noticeable for higher deformation rates.

Recent results concerning in situ AFM observation of corroded surfaces under strain in a chloride media will be presented.

Keywords : in-situ AFM, stainless steel, stress corrosion, chloride media, dislocations

Back

INTRODUCTION

For evident economic reasons, the study of localised corrosion of steels in aggressive media is crucial. For over 50 years it has been investigated and now the kinetics of pitting and stress-induced corrosion have become closer defined.

Corrosion as well as metallurgy and mechanical characterisation of stainless steels have intensely been studied by electronic microscopy (SEM, TEM) and classical electrochemical ways. These investigation techniques do not give an accurate look of the very first steps in the mechanism of localised corrosion because they do not gather in the same device the possibility to closely cartography the surface and to be in a liquid corrosive medium.

With the advent of local probe microscopy like Scanning Tunnelling Microscopy (STM) and Atomic Force Microscopy (AFM) 20 years ago [1], in-situ studies of corrosion has become possible. In metallurgy indeed, STM and AFM have proved to be very useful tools to study steels. The morphology of phases like martensite or of precipitates have been investigated by air STM. The atomic structure of passive films on austenitic steel [2], pure iron [3] or pure chromium [4] have been imaged by STM. Surface effects of plastic deformation on steels have also been analysed by these local probe microscopies [5]. In-situ AFM studies have been carried out on pitting corrosion of stainless steels and show the relationship between pits and precipitates on the surface [6,7,8].To our knowledge, in-situ stress-induced corrosion of stainless steels has never been studied by AFM. This article will relate the first attempts to fill this gap.

This paper reports the first results of an in-situ AFM study of localised corrosion (pitting and stress-induced corrosion) of a 304L stainless steel. Therefore an original set-up including an AFM, a traction device and an electrochemical cell has been developed.

EXPERIMENTAL METHOD

The original set-up developed in the laboratory needed to take in account many constraints: the sample itself had to be shaped to answer the drastic criteria of the study and the system has been designed with respect to the congestion due to every component, which are not compressible. It consists in the assembly of an Atomic force Microscope, a traction device and an electrochemical cell.

1. Sample

A 304L stainless steel was used in this work with the following chemical composition (wt%):

C	Mn	S	Ni	Cr	Mo	N	Cu	Fe
0.018	1.72	0.0005	10.14	18.68	0.35	0.072	0.15	balance

The shape of the test pieces is determined by three main points: 1) the room given to the sample in the set-up, 2) the fact that the strains must be localised under the scanning area (max 100x100 μm^2), 3) the possibility to adapt an electrochemical cell to the sample. Therefore the strains in samples with different shapes have been simulated with CATIA V.5 [9] and the definitive design of the test pieces are shown in Fig.1. The test pieces are rectangular (57x19x0.8 mm^3) with two holes in order to concentrate the stress in a small area. After machining, they were polished mechanically by SiC grains and diamond paste until 3µm grain size, then polished chemical-mechanically with colloidal silica from STRUERS

(40 nm particle size) during 20 hours. They were washed in distilled water, then in ethyl alcohol with ultrasonic stirring and dried with N_2. The austenitic (fcc) grain structure was completely revealed by the chemical-mechanical polishing. The typical corrugation (RMS) of the surface was about 1 Å for areas of at least 1 µm².

Description of the set-up:

The Atomic Force Microscope (AFM) used is a Picoscan II from Molecular Imaging. It is used in contact mode. It is placed in a "stand-alone" configuration above a "line-hole-plane" disc to insure a good stability and reproducibility of the position of the scanner. The traction device is fixed to the base of the set-up via a vernier X-Y translation platform to position the sample under the AFM tip. The electrochemical cell is fixed to the test piece, which is attached to the jaws of the traction device. A general scheme of the set-up is presented in Fig.2.

Concerning the electrochemical cell, notice that the working electrode (WE) is the sample and that the counter electrode (CE) is a silver wire, which is also used as a pseudo reference. The potential is applied and controlled by a GAMRY interface. The solution used is a borate buffer ($[H_3BO_3]$=0.1 mol/L, [borax]=0.002 mol/L) with different concentrations of NaCl, pH buffered at 7.5. The whole experiment was made at room temperature (20°C).

The traction device (Deben 5000N) stretches the sample at constant speed (0.02 mm/min) while the total force is measured.

The scanning area is localised with a CDD camera focalised on the AFM tip and the sample (that is the whole system sample + electrochemical cell + traction device) is moved until the tip is pointed to the area between the two holes, in the strain concentrating zone of the test piece.

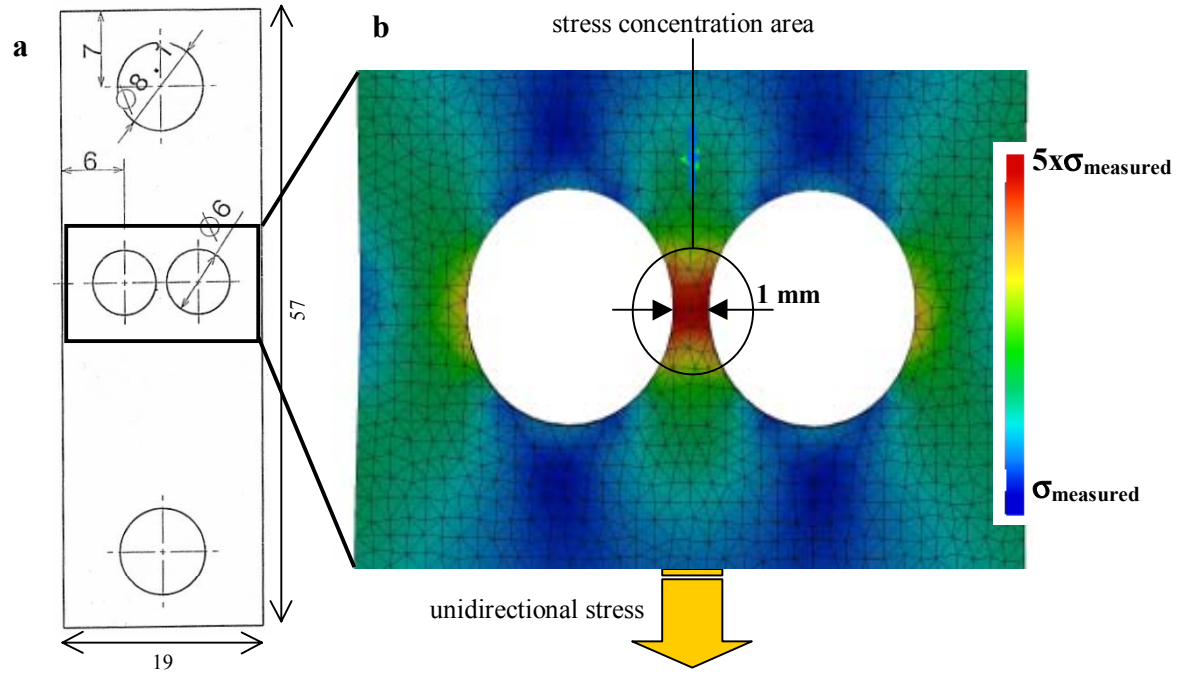

Fig. 1. Test piece shape and dimensions (mm) (a), and strain simulation with CATIA V.5 (b). It shows the concentration of stress in a very small area for this conformation of the sample. The force applied is 350N. The figure shows the final state of the test piece.

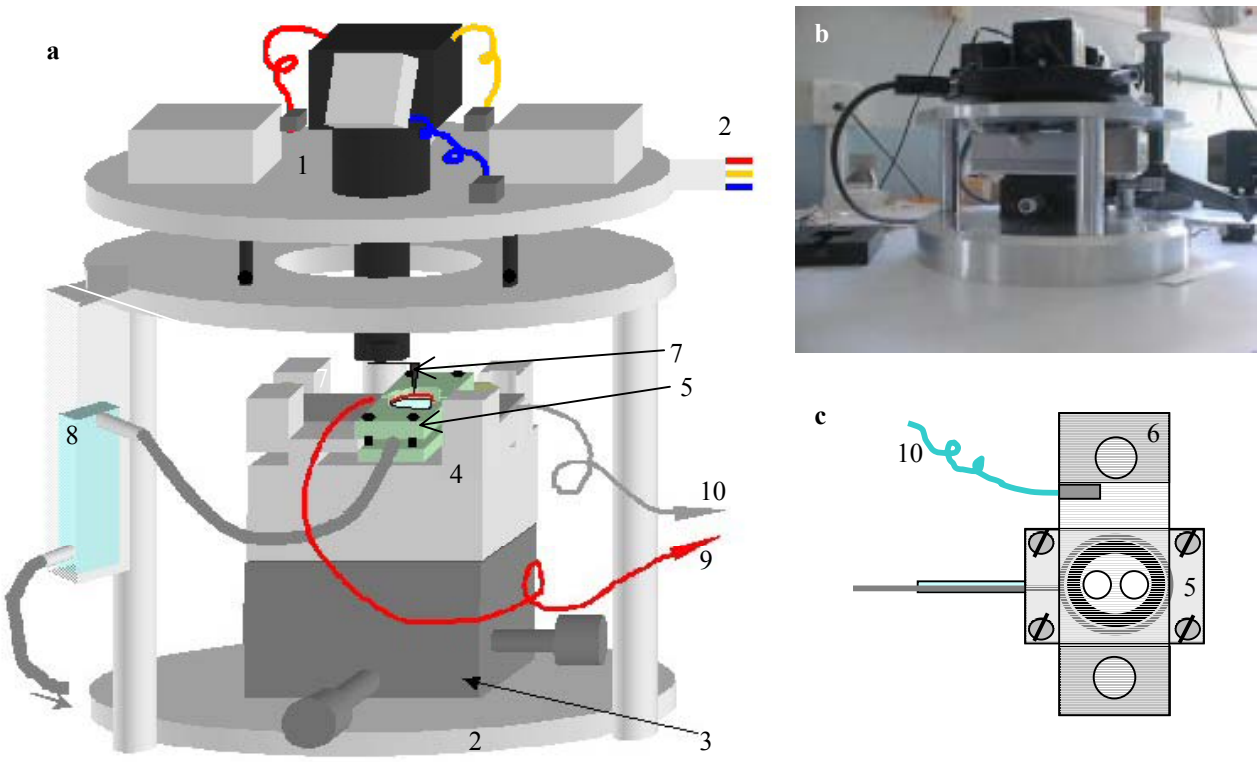

Fig. 2. a) general scheme of the set-up. 1, AFM head from Molecular Imaging in "stand-alone" configuration. 2, base isolated from high frequency vibrations. 3, X-Y vernier. 4, traction plate. 5, electrochemical cell. 6, sample. 7, AFM tip. 8, aqueous solution reservoir. 9, silver wire (CE). 10, copper wire connected to the test piece. b) picture of the experimental apparatus (scale 1:10). c) upper view of the electrochemical cell mounted on the sample.

RESULTS AND DISCUSSION

This study is divided in three parts to validate two by two the techniques associated in the set-up. The first one consists in the evaluation of the ability of the system to scan and cartography the surface during a traction test. The second part is dedicated to electrochemical behaviour of the 304L test pieces in corrosive solution, and in the last one, results obtained in-situ with AFM in solution during traction will be presented.

In-situ AFM scanning during traction in air

The experiment has been operated in air at room temperature. Because of the configuration of the system (test piece fixed at one end and stress applied to the other end), the scanned area moves during traction. As a consequence, a step by step traction is necessary to avoid losing it. The traction speed is 0.02 mm/min. After each step the tip is approached and the same area than before is scanned. The result of this traction observed by AFM is shown in Fig.3. It should be noticed that the force value on the curve is the measured value, which corresponds to the fifth of the strain applied to the sample in the area observed. Furthermore, the spikes observed on the traction curve (see arrows) are due to relaxation of the jaws of the traction system while scanning with the AFM and depend on the scanning duration.

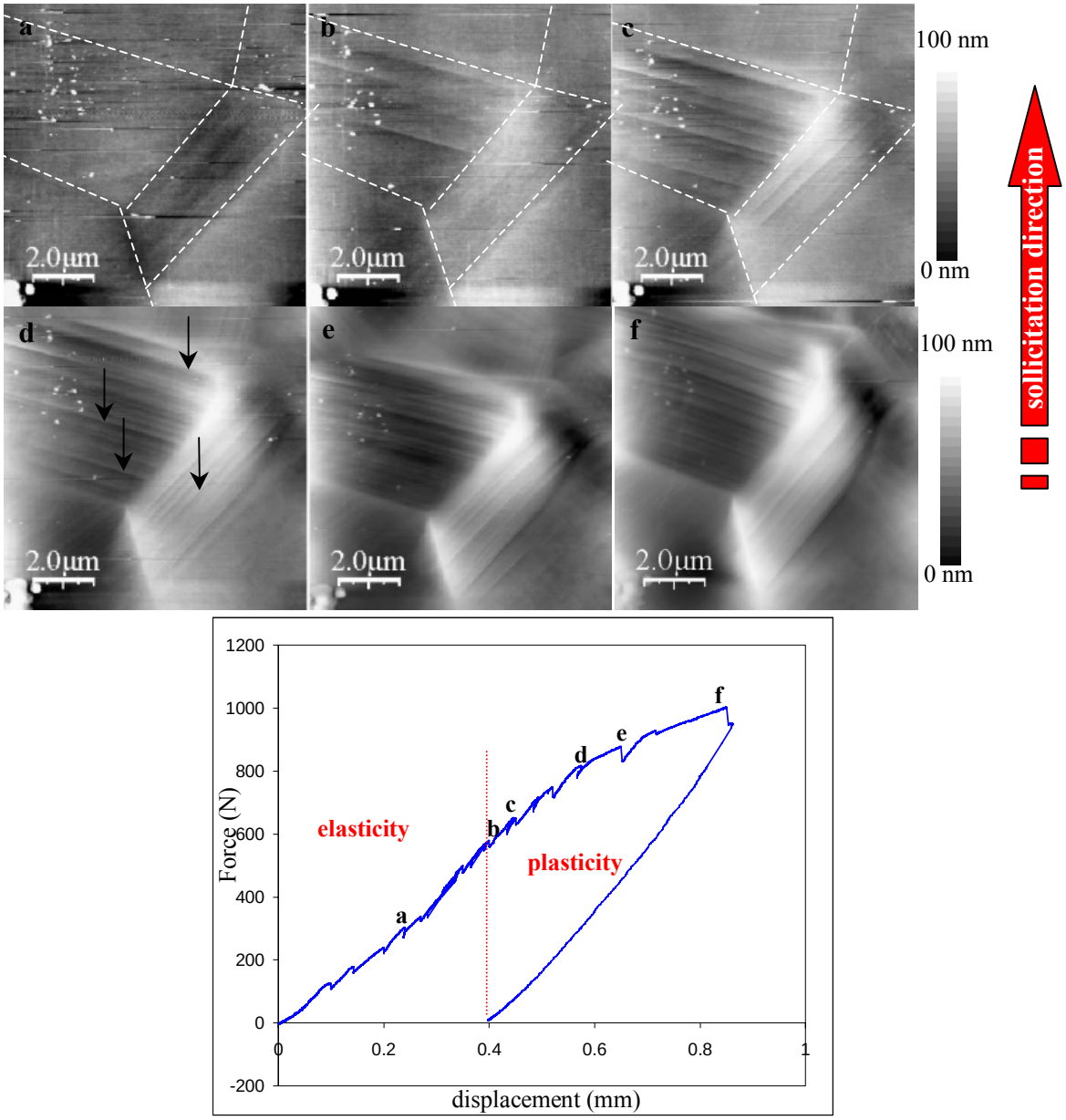

Fig. 3. Topographic images of the same area during traction obtained in contact mode AFM and corresponding traction curve. The letters a,b,c,d,e,f correspond to different deformations in the traction curve. While a) is still in the elastic domain, b,c,d,e,and f belong to the plastic domain. At least 6 grains can be seen on the images, delimited here by dashed white lines. The arrows in d) point out the slip lines.

First of all, Fig.3 shows clearly that the grain structure has been revealed by the mechanical-chemical polishing, which may have dissolved preferentially certain orientations of grains. At least six different grains can be enumerated on the images (dashed lines). When the sample is stretched, lines appear inside grains. These lines are all parallel to each other inside a same grain. This happens when the elastic limit of the test piece is over-passed in the scanning zone. These lines are actually steps with a typical height of 2 nm and correspond to slip planes emerging at the surface of the grains. When the deformation rate increases, the density of such slip lines increases also. It is assumed that the sample being made of an austenitic stainless steel with a fcc crystallographic structure, the slip planes are the dense

planes (111) [10,11]. This explains why the slip lines are parallel to each other inside one grain and have different orientation from grain to grain.

Above a certain stress applied to the sample, which is around 800 N as measured on Fig.3, the emerging of another slip plane system occurs inside grains (Fig.4). It is then supposed that the stress at this moment is strong enough to liberate a new and tighter slip system instead of carrying on developing the first one. It is assumed that this secondary slip plane system should belong to the (111) plane type (another one with a direction hardly solicited considering the general stress direction) or to the (110) plane type. At this deformation rate, two slip plane systems are active to ensure the plastic deformation.

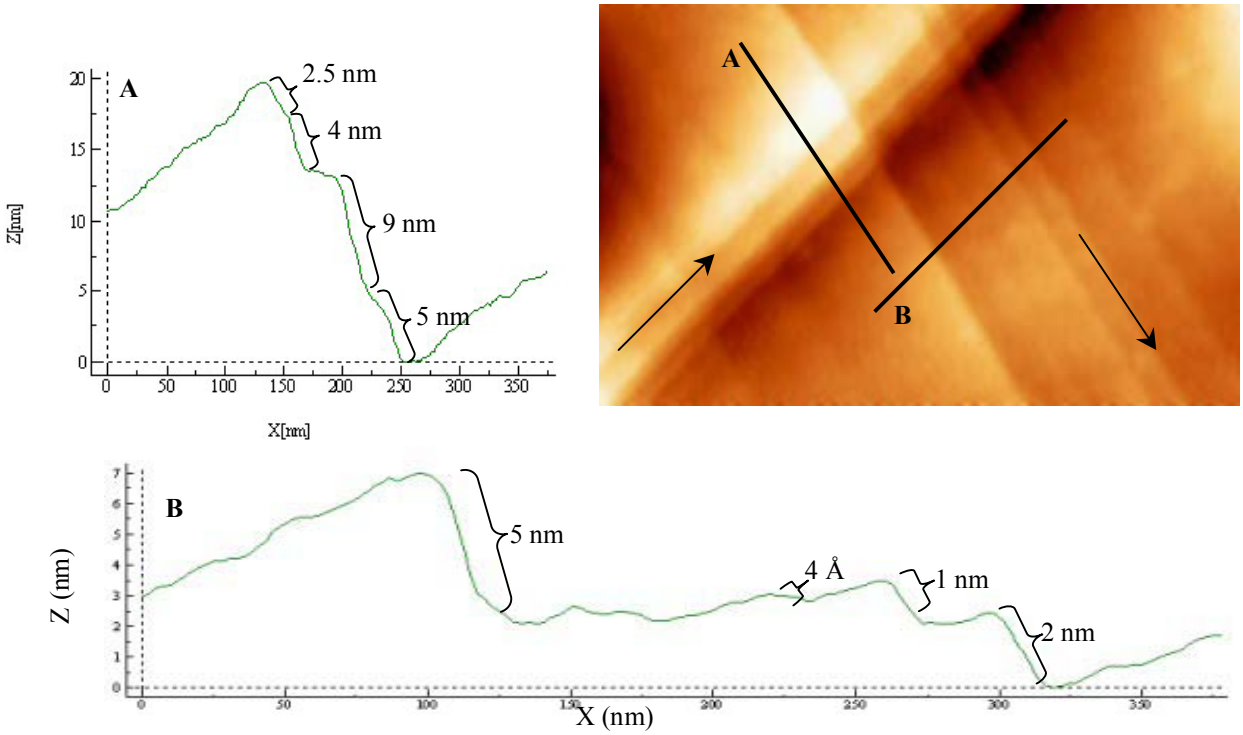

Fig. 4. Topographic contact AFM image of the surface inside a grain. The arrows indicate the trace of the slip planes: 2 different orientations. The profiles A and B taken along the lines A and B respectively show steps, which height can vary between 4 Å and 9 nm.

Figure 4 shows also the high vertical resolution of the set-up: a step 4 Å high can be imaged, which corresponds to few (2 or 3) Bürgers vectors translations. At the very best it would be possible to make the system able to image a step formed by one Bürgers vector translation. This confirms the choices made during conception of the set-up.

If the sample is brought to a higher stress (Fig.5), the strain fields are strong enough to rotate the grains and the step emerging almost stops in favour of this grain loosening.

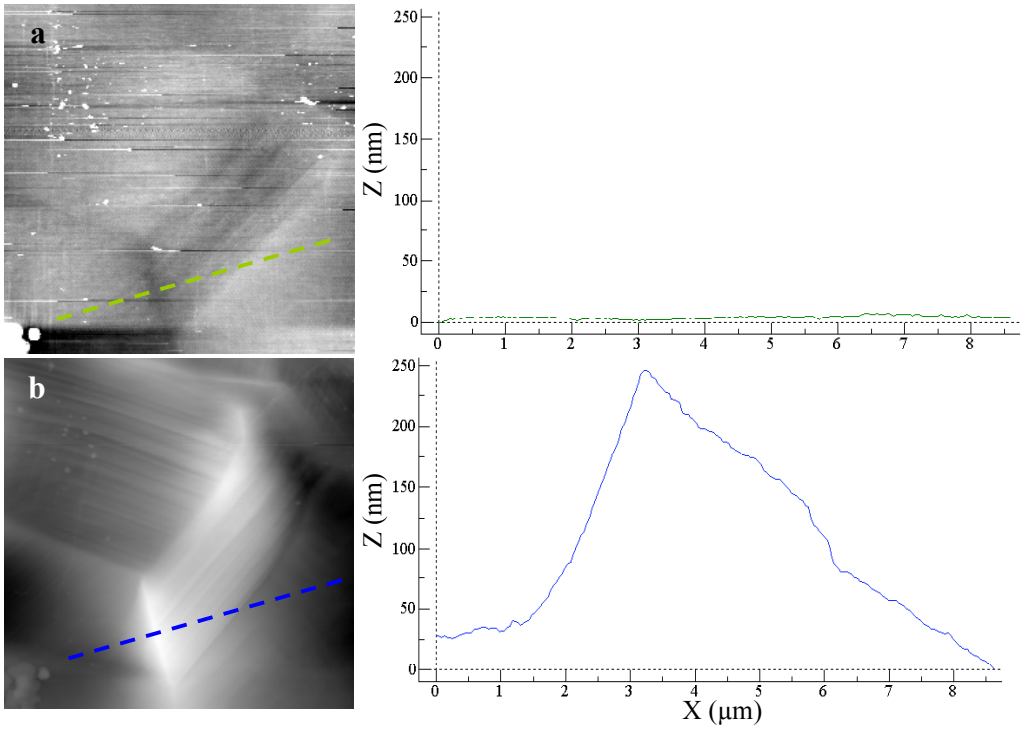

Fig. 5. Topographic contact AFM images of the surface before (a) and after (b) high deformation rate (40% for b) and profiles drawn along the dashed lines. The blue profile shows different slopes from grain to grain after a high deformation: grain loosening has occurred.

All these observations are consistent with results obtained with an AFM in air after nano-indentation [12].

For the next studies, the traction has been stopped before the grain loosening.

304L Stainless steel immersed in chloride solution

In this experiment, a sample was simply immersed in the borate buffer solution with different concentrations of chloride, waiting for free pitting corrosion to initiate. The free corrosion potential of the stainless steel was measured and then applied to it for hours or days. At the same time, the same area of the sample was scanned with the AFM at different times and the intensity of the current between the sample and the CE was recorded. Pitting corrosion is a well known stochastic phenomenon [13,14,15,16]. At macroscopic scales, pitting occurs after weeks in those conditions and seems not to be accelerated by the Cl^- concentration at room temperature. In order to avoid degradation of the AFM head, which is immersed in the corrosive solution too, in-situ investigations cannot be pursued beyond three full days. The concentrations of NaCL used were 9, 20,30,50,70 and 100 g/L. In any case we did not notice a change at nanometric scale in the outer structure of the stainless steel on ten different areas (100x100 µm²) of the sample. It is due to the fact that at free corrosion potential the 304L stainless steel holds itself at about 300-400mV under the pitting potential evaluated from cyclic polarisations (this recording is in good agreement with results previously published in literature [17,18]). The cyclic polarisation curve (Fig.6) obtained in borate buffer solution, [NaCl]=9g/L, confirms it. Speed scan was 0.1 mV/s.

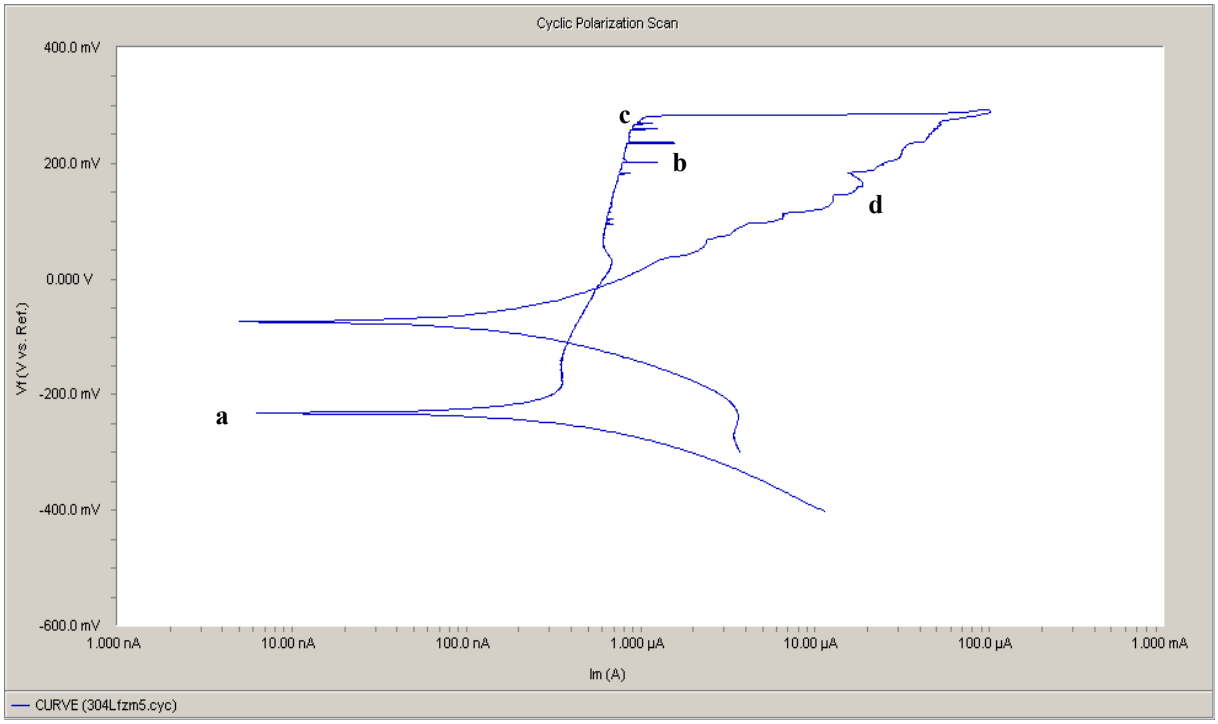

Fig. 6. Cyclic polarisation scan of the 304L polished sample in aqueous borate buffer solution containing 9g/L of NaCl, at room temperature. a) corrosion potential. b) electrochemical noise before pitting (depassivation / passivation cycles). c) pitting potential. d) return.

Now, the objective is to hold the potential close to the electrochemical noise and observe what happens with or without traction of the test piece in solution. First experiments made without stress have revealed difficulties: for potential applied to the sample too close to the pitting potential, unexpected pitting appears and chromium oxides create bichromates. These compounds precipitate and strongly perturb the measurements of the AFM cantilever position.

In-situ AFM scanning during traction in chloride solution

Since the difficulties encountered for AFM-scanning and controlling the potential at the same time by an electrochemical way have not yet been dismissed, the experiments have been carried out at open circuit potential, that is at the corrosion potential of the system (sample + CE/Ref). The solution was an aqueous borate buffer, pH=7.5, with [NaCl]=1mol/L. During AFM scanning, the solution was left open to air at ambient temperature.

A three steps traction has been done, until the plastic domain was reached, with about 1 hour left in between each step in order to scan the proper area and to let time to the electrochemical system to stabilise. The traction curves were very similar to the one obtained in air and the quality of the AFM imaging in solution was preserved. Figure 7 sums up the experiment.

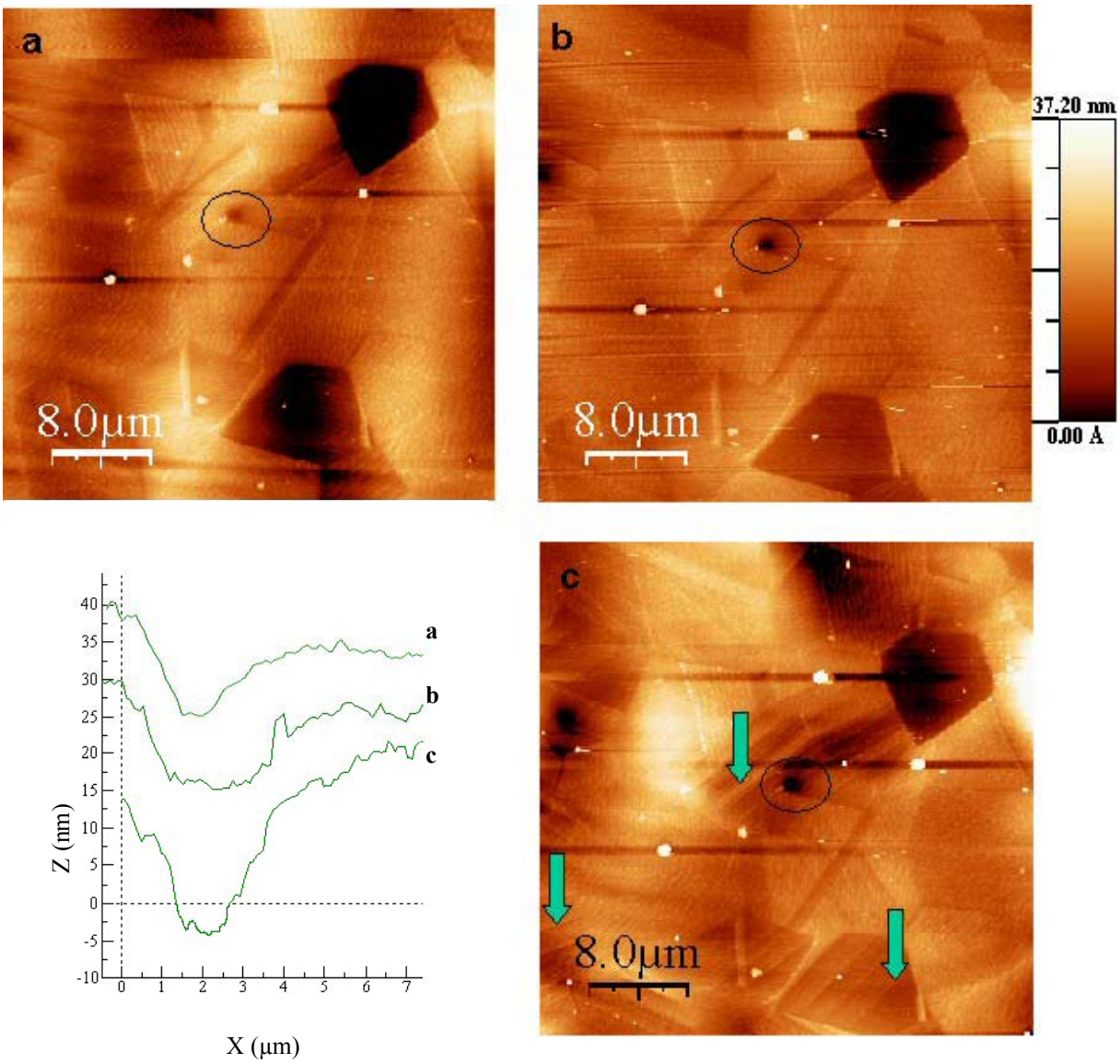

Fig. 7. Evolution of the topography of the surface during traction (same traction curve than in air) at each step a, b and c. a) and b) are still in the elastic domain whereas c) is in the plastic one. The rings and the horizontal profiles corresponding show the pitting propagation of a pre-existent pit and the arrows show the slip lines in the grains. The z-scale is the same in all 3 images.

This experiment shows mainly three features: the limit of elasticity is the same even with the electrochemical cell, which could harden the system, and the set-up is valuable for such an in-situ study.

Slip lines are clearly visible and are not preferentially attacked by the chloride medium. This is essentially due to the very low duration of the experiment: the stochastic phenomenon of pitting or stress corrosion had not enough time to incubate before the scan was made.

The chloride solution is corrosive enough to enable pitting propagation on a pre-existing pit. The deepness of the pit indeed increases with time exposure to the solution. This pit, initiated during the mechanical-chemical polishing, is probably located around an impurity let on the surface.

Back

CONCLUSION

These first observations show that AFM enables us to study local corrosion phenomena in detail. The set-up presented here gathers all the qualities required for an in-situ investigation of stress-induced corrosion.

The set-up is now operational and presents a very good resolution at the nanoscale. It has proved its efficiency for the observation of the nanometric surface modifications during traction in chloride solutions: 4 Å high slip planes are visible, pitting can clearly be observed in-situ and the potential of the sample controlled.

Hence a complementary in-situ study of corrosion induced by stress in chloride solution is in progress by adjusting the potential of the sample.

REFERENCES

1. Binnig G., Rohrer H., Gerber C. and Weibel E., *Phys. Rev. Lett.* **49** (1982) 57
2. Olive J.M. and Vignal V., *Microsc. Microanal. Microstruct.* **5** (1994) 301
3. Ryan M.P., Newman R.C. and Thomson G.E., *J. Electrochem. Soc.* **142** (1995) L177
4. Maurice V., Cadot S. and Marcus P., *Surface Science* **458** (2000) 195
5. Olsson C.-O.A. and Landolt D., *Electrochim. Acta* **48** (2003) 1093
6. Reynaud-Laporte I., Vayer M., Kauffmann J.P. and Erre R., *Microsc. Microanal. Microstruct.* **8** (1997) 175
7. De Wit J.H.W., *Electrochim. Acta* **46** (2001) 3641
8. Leblanc P. and Frankel G.S., *J. Electrochem. Soc.* **149** (6) (2002) B239
9. CATIA V5 is a property of Dassault Systemes
10. Villechaise P., Sabatier L. and Girard J.C., *Mater. Sci. Eng.* **A323** (2002) 377
11. Man J. et al., *Mater. Sci. Eng.* **A351** (2003) 123
12. Koch G.H., Agrawal A.K., Brongers M.P.H., Phelps A.W., *CORROSION 99* 450
13. Shibata T. and Takeyama T., *Corrosion* **33** (1977) 243
14. Macdonald Digby D. and Urquidi-Macdonald M., *Electrochim. Acta* **31** (1986) 1079
15. Vera Cruz R.P., Nishikata A and Tsuru T., *Corrosion Science* **40** (1998) 125
16. Park J.-J and Pyun S.-I., *Corrosion Science* **46** (2004) 1469
17. Bastidas J.M. et al., *Corrosion Science* **44** (2002) 625
18. Phadmis S.V. et al., *Corrosion Science* **45** (2003) 2467